machines

MDPI

Article

An Almost Comprehensive Approach for the Choice of Motor and Transmission in Mechatronic Applications: Torque Peak of the Motor

Giancarlo Cusimano * and Federico Casolo

Department of Mechanics, Politecnico di Milano, Via Giuseppe la Masa 1, 20156 Milan, Italy; federico.casolo@polimi.it

* Correspondence: giancarlo.cusimano@polimi.it; Tel.: +39-2-2399-8439

Abstract: The choice of motor and transmission to move a joint must ensure that the torque peaks of the motor lie inside its dynamic operating range. With this aim, this paper proposes an approach in which all the candidate transmissions are processed one by one to find among all the candidate motors those they could execute the reference task with. Consequently, all the transmission parameters, and not only its transmission ratio, are taken into consideration in advance. For rectangular dynamic operating ranges, this approach allows a direct and precise evaluation of all the admissible motor-transmission couples, without any approximation and further check. Apart from an entirely automated procedure, the method also provides diagrams through which the designer can concisely compare the admissible solutions. Furthermore, the method provides a solution for the drive systems in which the limit torque of the dynamic operating range does depend on the motor speed.

Keywords: motor-transmission coupling; servo-motor; dynamic operating range; transmission efficiency; power flow alternation; transmission inertia

Citation: Cusimano, G.; Casolo, F. An Almost Comprehensive Approach for the Choice of Motor and Transmission in Mechatronic Applications: Torque Peak of the Motor. *Machines* **2021**, *9*, 159. https://doi.org/10.3390/machines9080159

Academic Editor: Christoph Hackl

Received: 17 June 2021
Accepted: 3 August 2021
Published: 8 August 2021

1. Introduction

In mechatronic applications the choice of motor and transmission must take into account two main issues concerning the motor, its thermal problem and its torque peak problem, to be considered in parallel. As for the latter, during the working cycle, the drive system must often exert considerable torque peaks to balance high resistant and inertia loads acting in small time ranges. These torque peaks must be allowed by the dynamic operating range of the drive system.

The interposition of the transmission between motor and load makes the problem more complex and interesting for many reasons. First, the transmission ratio τ reduces the motor speed and amplifies the motor torque on load side. Second, the direct and inverse transmission efficiencies, denoted by η_d and η_i, respectively, modify the required motor torque. Third, sometimes the transmission inertia $J_{T,M}$ on motor side and $J_{T,L}$ on load side significantly increase the inertia torque. Fourth, the transmission speed limit $\omega_{T,M,max}$ on motor side and the torque limit $M_{T,L,max}$ on load side impose two constraints that must be respected.

The complexity of the problem requires the simultaneous choice of drive system and transmission according to different methods described in the technical literature.

Some papers regard the drive train optimization for industrial robots, for which a concurrent design approach is required in order to take into consideration the reciprocal effect of the different drive trains. Both the thermal problem and the torque peak problem of the motor are taken into account. The optimization requires a complete model of the robot and an adequate model of transmission and drive system. The optimal motor-reducer couple is found by minimizing a single or multi-objective criterion. A multi-objective optimization permits a good compromise among different requirements regarding both the

general characteristics of the machine (cost, weight etc.) and its performances, as shown in the following works. Roos et al. [1] compared the drive system-transmission couples able to perform the reference task by means of suitable diagrams for the minimization of the different objective functions. Petterson et al. [2] considered a model of the motor in which all the parameters are continuous functions of the design variables (length and radius of the motor), while the transmission parameters depend on a discrete number of its size. The optimization results are the motors and transmissions that minimize the global cost while respect the performance requirements. Zhou et al. [3] studied the optimization of the drive trains of a light-weight robot. Motors and transmissions, taken from a limited catalog, are simultaneously optimized for the different axes. Ge et al. [4] carried out the optimal choice of motors and transmissions among available components by means of dynamic optimization, with an objective function made up of working efficiency and natural frequency. Padilla-Garcia et al. [5] introduced an electro-mechanical model of the motors that allows the designer to obtain the dynamics of the robot. The transmissions are assigned. A genetic algorithm allows the choice of off the shelf servomotors and the tuning of the control gains, with an objective function that minimizes tracking error, global weight of the motors and energy consumption.

More recent papers concern mobile robots and/or robots with compliant actuators with particular reference to the energy efficiency. For non-linear dynamics, Nasiri et al. [6], proposed to adapt non-linear compliances in order to minimize a cyclic energy consumption. For robots interacting with men, Verstraten et al. [7] analyzed the effect of series elastic actuators and parallel elastic actuators for an often-relevant minimization of the power peak and the energy consumption. Haddadin et al. [8] compared motors with elastic joints with motors with rigid joints, both reaching the same maximum speed, in order to find the mass decrease of the first solution. For robot applications, Saerens et al. [9] studied scaling laws for different transmission types in view of a multi-variable optimization, and found the influence of diameter, length, transmission ratio and number of stages on the maximum continuous output torque and the generalized inertia on load side. Saerens et al. [10] conducted a similar study for different types of springs for compliant actuators in view of their energy storage capacity. In all these works, the efficiency of the transmission is considered in an approximate way.

Some papers concern the selection of drive system and transmission when the motor must be modelized with an internal viscous torque due to the iron losses. Particular attention is paid to the energy efficiency. In particular, Rezazadeh et al. [11] proposed a method for the choice of the motor-transmission couple based on the minimization of the total energy for a given reference task and on the minimization of the bandwidth as a second objective function. For a mobile robot, Verstraten et al. [12] proposed a model of motor and transmission in order to evaluate the mechanical and electrical energy losses, and provided a series of recommendations in this regard. Verstraten et al. [13] compared different models for the prediction of the energy consumption of a DC motor-transmission couple, and underlined the relevance of the power flow direction in this regard. Bartlett et al. [14] proposed a method for the optimal choice of the transmission ratio in terms of rms motor torque and rms electrical power, taking into account the saturation and the thermal limits of the drive system.

In a more classical approach, a single axis is taken into account, and there is a distinction between two phases. A first feasibility phase allows the designer to find all the admissible drive system-transmission pairs with respect to a specified reference task; it should be followed by an optimization phase, which allows the designer to find, among those admissible, the drive system-transmission couple that minimizes additional criteria. Normally, these papers stop at the first phase. The present paper adopts this approach.

Some papers [15–18] take into account the complete set of the motor characteristics, whereas they only consider the main parameter of the speed reducer, i.e., the transmission ratio τ. Sometimes, these papers only deal with the motor thermal problem, other times only with the torque peak problem and other times with both of them. Nevertheless, all

the systems must be further checked, taking into consideration the complete set of the transmission characteristics: hence, only after this second step, the admissibility of the drive system-transmission couple can be ensured.

Other papers [19–25] take into account the reducer efficiency from the outset.

The method introduced by Van de Straete [16] is extended by Giberti et al. [19,20]. They considered the motor thermal problem and both the direct and inverse transmission efficiency. However, on the one hand, these parameters are constant, and on the other hand, during the reference task, the power flow through the speed reducer is unidirectional, either direct or inverse. With this approach, some admissible drive system-transmission couples can be improperly excluded.

Generally, in mechatronic applications, the power flow through the reducer changes its direction, generating an alternation of the direct and inverse transmission efficiency; just think of the inertia forces of the load. In general, this condition increases the set of the admissible motor–transmission couples. Cusimano [21,22] introduced the alternation of the mechanical power flow through the transmission. He studied the choice of the motor-transmission couple with reference to a rectangular dynamic operating range.

The case of a non-rectangular dynamic operating range of the drive system is dealt with by Cusimano [23,24]. The first work shows how the choice method proposed in [16,19] can be applied to this case, whereas paper [24] presents a new and more complete approach.

With reference to the motor thermal problem, Cusimano et al. [25] proposed a method in which each candidate transmission is singularly taken into consideration. The first step is to check if it is able to move the load according to its speed and torque limits, i.e., if it is admissible. Then, for each admissible transmission, the second step is to find all the drive systems that can be coupled with it in order to execute the reference task from the point of view of the thermal problem of the motor. Thus, it is possible to find all the motors that can be coupled with a given transmission without the need of a further check. The motors taken into account present a nearly horizontal limit curve of their continuous duty operating range S1.

The present work deals with the problem of the torque peak of the motor, and its rationale is to consider the candidate transmissions one by one; hence, all their parameters are known from the outset. Following a path similar to that traced in [25], not only all the drive system parameters but also all the transmission parameters are taken into account from the beginning: therefore, all the candidate drive systems that can be coupled with each candidate transmission are definitively determined, without the need of a further check. To this aim, a completely automated procedure is used. Furthermore, the work presents the guidelines to draw new diagrams that allow the designer to compare the admissible drive system-transmission pairs. Initially the authors consider motors with a nearly horizontal limit curve of their continuous duty operating range and a horizontal limit curve of their dynamic operating range. Afterwards, they also consider motors with a different shape of these operating ranges.

In particular, in this paper, Section 2 explains the load specifications and indicates the inequalities due to the constraints regarding both transmission and motor. Section 3 considers a given speed reducer and checks if it must be excluded according to the corresponding inequalities; otherwise, it introduces an automated procedure to find the admissible drive system-transmission couples when the dynamic operating range can be considered rectangular. For each admissible speed reducer, Section 4 introduces new diagrams in order to find and compare the drive systems that are able to exert the required torque peaks of the motor. In Section 5, an industrial case study is analyzed. Section 6 solves the torque peak problem for drive systems that show a non-rectangular dynamic operating range: for many of them, the procedure is similar to that applied when the dynamic operating range is rectangular; for the remaining ones, a more complex method is explained. Section 7 shows how the proposed procedure can be applied to motors with an internal viscous torque. Section 8 discusses the conclusions.

2. Specifications

Figure 1 shows the first quadrant of the dynamic operating range of a permanent magnet brushless motor.

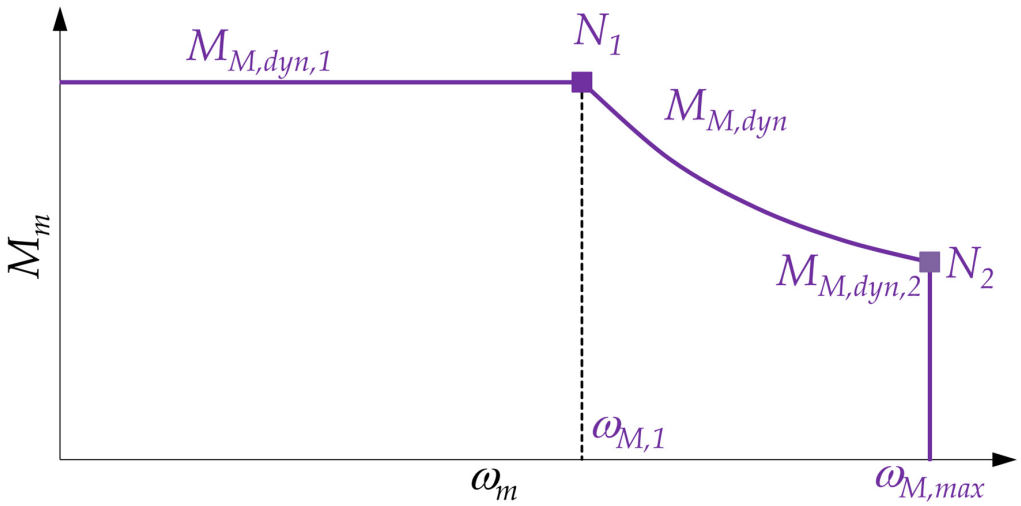

Figure 1. Dynamic operating range of the drive system.

Denoting the motor torque by M_m and its speed by ω_m, in the ω_m-M_m plane, the dynamic operating range is limited by the motor maximum speed $\omega_{M,max}$ and by a variable torque $M_{M,dyn}$, due to the electronic drive feeding the motor. As far as speed $\omega_{M,1}$, at which the voltage saturates, $M_{M,dyn}$ is constant. Beyond $\omega_{M,1}$, there is a descending profile of $M_{M,dyn}(\omega_m)$. At a given speed ω_m, if the required motor torque M_m should be higher than $M_{M,dyn}(\omega_m)$, the electronic drive would not allow the motor to exert it, so that the machine would not work properly: this is the torque peak problem.

Figure 2 shows the scheme of a machine. For the choice of motor and transmission suitable to move a joint only the corresponding degree of freedom of the machine is taken into consideration, whereas the effects of other degrees of freedom are included in the load torque M_l exerted on the joint. This torque includes both inertia and resistant loads.

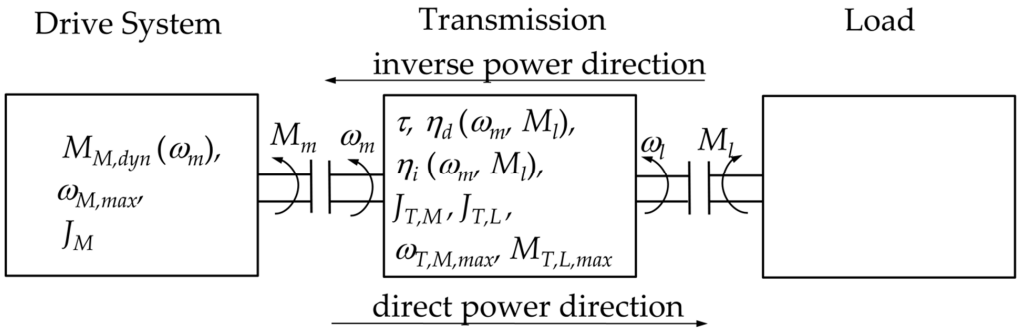

Figure 2. Scheme of a machine.

In this paper, the drive system operating ranges are assumed to be symmetrical in the four quadrants. A simple dynamic operating range of the brushless motor is initially used, with a constant torque denoted by $M_{M,dyn}$ (Figure 3). This is a common assumption because the motor speed often does not exceed $\omega_{M,1}$. However, later, for the drive systems in which the limit torque of the dynamic operating range does depend on the motor speed, Section 6 will explain how to solve the issue for many of them, by means of a procedure similar to that applied when $M_{M,dyn}$ is constant and also explains how to fix the problem for the remaining drive systems, by means of a more complex method.

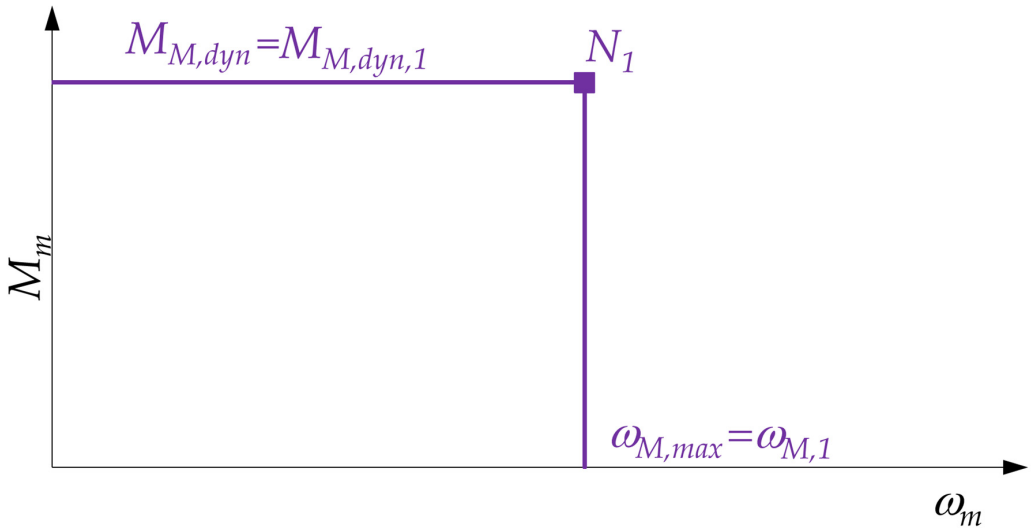

Figure 3. Simplified dynamic operating range of the drive system.

The specification of the load reference task allows the designer to know the joint angular speed $\omega_l(t)$ and acceleration $\alpha_l(t)$ as functions of time, together with the load torque $M_l(t)$. In general, a numerical simulation, in which the motor and transmission sought are not included, provides these quantities.

3. The Method of Starting from a Given Transmission

Although the authors also appreciate other approaches, they observe that starting from a given transmission allows the designer to take into account all its functional and constraint parameters from the outset, which avoids any further check. In addition, assuming that the motor perfectly performs the reference task, it is possible to directly discard the gearboxes that do not allow it to be done. In general, with this approach, it is not possible to represent the parameters of the gearboxes as continuous functions of their design variables in order to proceed with an optimization.

Incidentally, it is easy to introduce among the various real transmissions a fictitious one that corresponds to the direct coupling between motor and load. It is also simple to consider an equivalent transmission that is made up of two real transmissions in series.

Once a transmission is taken into consideration, many ways of proceeding open to the designer. For the sake of simplicity, in this section this paper continues as in [25] and finds the motors (with a rectangular dynamic operating range and in which the iron losses are negligible) that can be coupled with the given transmission, taken from a catalog, in order to perform the reference task from the point of view of the torque peak of the motor.

3.1. Admissible Transmissions

A candidate transmission is now taken into consideration, and therefore, all its parameters are known. As already explained in [25], the first step is to find the transmission torque on load side and then to check if its torque and speed limits allow the reducer to move the load during the reference task, i.e., if it is admissible.

Denoting by $J_{T,L}$ the moment of inertia of the transmission on load side, the transmission torque $\widetilde{M}_l$ on load side is a known function of time given by

$$\widetilde{M}_l(t) = M_l(t) + J_{T,L}\alpha_l(t)\ . \tag{1}$$

The maximum value $\omega_{l,max}$ of the transmission speed on load side is

$$\omega_{l,max} = \max_t[|\omega_l(t)|] \tag{2}$$

or is a specification higher than the value given by Equation (2).

Obviously, the transmission speed on motor side, that is the motor speed $\omega_m(t)$, is given by

$$\omega_m(t) = \frac{\omega_l(t)}{\tau} \tag{3}$$

The maximum absolute value $\widetilde{M}_{l,max}$ of $\widetilde{M}_l(t)$ is given by

$$\widetilde{M}_{l,max} = \max_t \left[\left| \widetilde{M}_l(t) \right| \right], \tag{4}$$

while the maximum absolute value $\omega_{m,max}$ of the motor speed $\omega_m(t)$ is given by

$$\omega_{m,max} = \max_t [|\omega_m(t)|] = \frac{\omega_{l,max}}{\tau} \tag{5}$$

Therefore, in order to be admissible, the speed reducer must meet the following set of inequalities:

$$\begin{cases} \widetilde{M}_{l,\max} \leq M_{T,L,\max} \\ \frac{\omega_{l,\max}}{\tau} \leq \omega_{T,M,\max} \cdot \end{cases} \tag{6}$$

If the given transmission is not admissible, it is discarded and a new speed reducer must be taken into account; otherwise, each of the candidate drive systems must be examined in order to check if it can be coupled with the given transmission to execute the reference task (from the point of view of the torque peak of the motor).

3.2. Admissible Drive System—Transmission Couples

Therefore, for an admissible transmission, a candidate drive system is now taken into consideration; it is characterized by its moment of inertia J_M, maximum speed $\omega_{M,max}$ and limit torque $M_{M,dyn}$ of its dynamic operating range. The torque peak of the motor must now be found. To this aim, it is necessary to introduce the following considerations involving the transmission parameters.

As explained in [21,22], the power flow through the transmission is direct if

$$\widetilde{M}_l(t) \cdot \omega_l(t) > 0 \tag{7}$$

and in this case, the direct efficiency η_d must be used, whereas the power flow is inverse if

$$\widetilde{M}_l(t) \cdot \omega_l(t) < 0 \tag{8}$$

and then, the inverse efficiency η_i must be considered.

Both efficiencies, η_d and η_i, can depend on the motor speed, and therefore also on the load speed, and on the load torque:

$$\begin{cases} \eta_d = \eta_d \left[\omega_l(t), \widetilde{M}_l(t) \right] \\ \eta_i = \eta_i \left[\omega_l(t), \widetilde{M}_l(t) \right]. \end{cases} \tag{9}$$

The effect of the transmission efficiencies is that, for the determination of the motor torque, instead of $\widetilde{M}_l(t)$, a different torque $\widetilde{M}'_l(t)$ must be considered on the load side of the transmission. If inequality (7) is met, it is given by

$$\widetilde{M}'_l(t) = \frac{\widetilde{M}_l(t)}{\eta_d \left[\omega_l(t), \widetilde{M}_l(t) \right]} \tag{10}$$

and in this case, it is amplified with respect to $\widetilde{M}_l(t)$; else, if inequality (8) is met, it is given by

$$\widetilde{M}'_l(t) = \eta_i \left[\omega_l(t), \widetilde{M}_l(t) \right] \cdot \widetilde{M}_l(t) \tag{11}$$

and it is reduced with respect to $\widetilde{M}_l(t)$. For a given transmission $\widetilde{M}'_l(t)$ is a known function of time.

Denoting by $J_{T,M}$ the moment of inertia of the transmission on motor side, the equilibrium equation of the system is expressed by

$$\frac{1}{\tau}M_m(t;J_M) = \frac{J_M + J_{T,M}}{\tau^2}\alpha_l(t) + \widetilde{M}'_l(t)\ . \tag{12}$$

As in [25], it is now convenient to define the torque $\hat{M}'_l(t)$ that also includes the known effect of the transmission inertia on motor side:

$$\hat{M}'_l(t) = \widetilde{M}'_l(t) + \frac{J_{T,M}}{\tau^2}\alpha_l(t)\ . \tag{13}$$

Moreover, $\hat{M}'_l(t)$ is a known function of time.

At last, the motor torque is equal to

$$M_m(t;\ J_M) = \frac{J_M}{\tau}\alpha_l(t) + \tau\hat{M}'_l(t) \tag{14}$$

It is noteworthy that $\alpha_l(t)$, $\hat{M}'_l(t)$ and τ are known because they only depend on the specifications and the given transmission. Consequently, on the right-hand side only J_M changes with the considered drive system.

The torque peak $M_{m,max}$ of the motor can now be found. In fact, the absolute value of the motor torque is given by

$$|M_m(t;\ J_M)| = \left| J_M\frac{\alpha_l(t)}{\tau} + \tau\hat{M}'_l(t)\right| \tag{15}$$

and $M_{m,max}$ is equal to

$$M_{m,max}(J_M) = \max_t[|M_m(t;\ J_M)|] \tag{16}$$

Therefore, a drive system can be coupled with the given transmission if it meets the following set of inequalities:

$$\begin{cases} M_{m,max}(J_M) \le M_{M,dyn} \\ \frac{\omega_{l,max}}{\tau} \le \omega_{M,max}. \end{cases} \tag{17}$$

Since J_M and $M_{M,dyn}$ are known for the motor into consideration, the calculation of its torque peak and the comparison with $M_{M,dyn}$ are simple, and thus, the first inequality is easily checked. The second inequality is immediately checked too. Figure 4 shows the flowchart of the whole procedure.

In this way, it is then possible to consider a feasibility matrix G whose generic element $g_{r,s}$ refers to the r-th transmission and the s-th drive system. If $g_{r,s}$ is equal to one, the s-th motor can be matched with the r-th transmission to carry out reference task of the load from the point of view of the torque peak of the motor; conversely, if it is equal to zero, the s-th motor and the r-th transmission, coupled together, cannot execute the reference task. Hence, this matrix concisely represents the result of the feasibility analysis from the perspective of the torque peak of the motor.

The motor thermal problem and the torque peak problem must be tackled together, by applying in parallel the two methods proposed in [25] and in this paper. The definitive set of admissible drive system-transmission pairs is the intersection between the two sets, separately found. Since a matrix F, similar to G, was filled in [25] for the motor thermal problem, it is clear that a logical AND between the two matrices provides a new matrix that shows all the drive system-transmission couples able to execute the reference task from both the points of view.

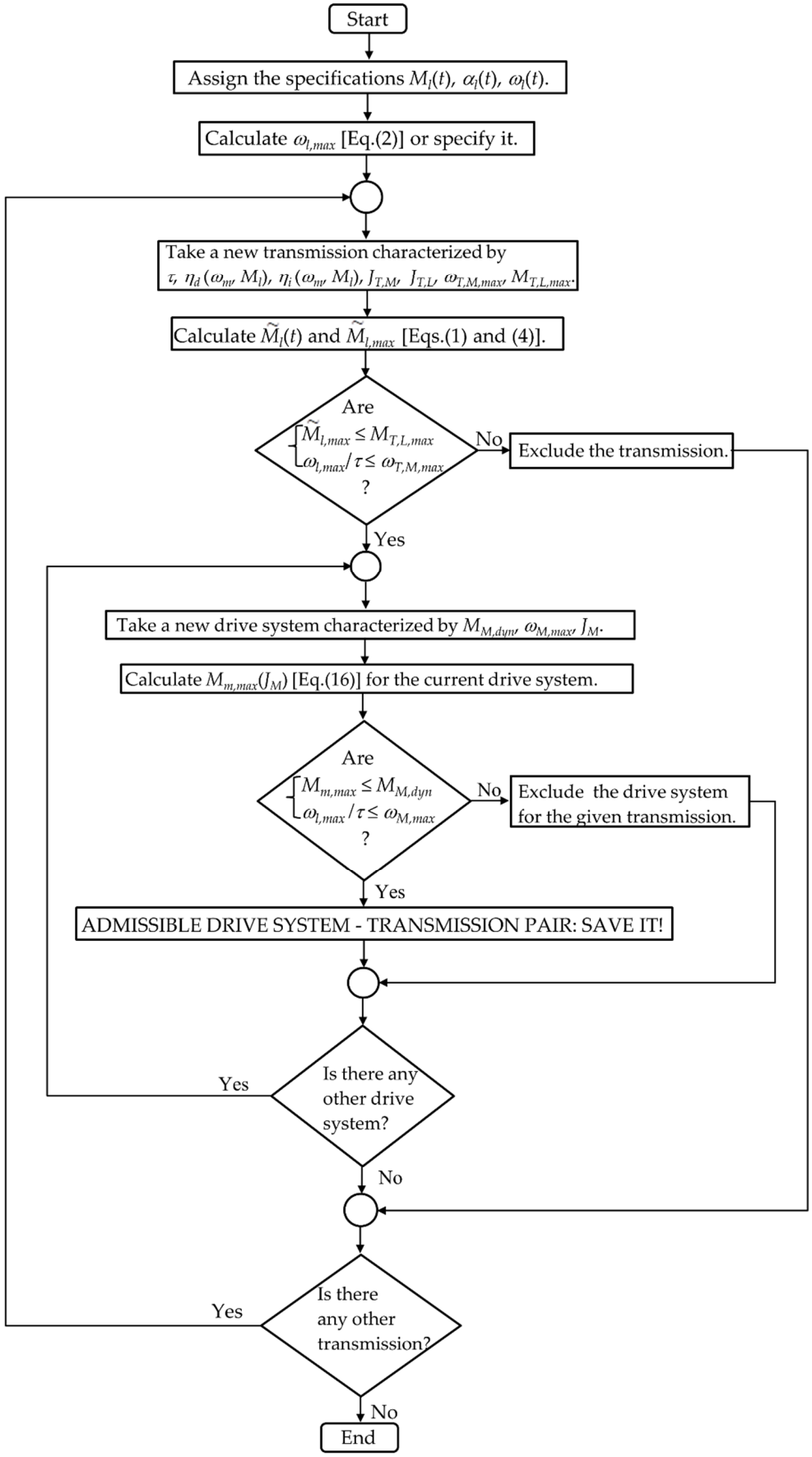

Figure 4. Flowchart of the automated procedure to find all the admissible motor–transmission couples.

It is clear that some of the admissible drive system-transmission couples can be discarded due to other constraints that need to be respected. Sometimes this exclusion can be done from the beginning. For instance, when the overall weight of electronic drive, motor and transmission must not exceed a given threshold.

Although the subsequent optimization phase is beyond the scope of this paper and dealt with in its entirety is a complex problem, it is possible to make some considerations in the hypothesis of finding among the admissible drive system-transmission pairs, whose number is discrete, the one that minimizes a given objective function.

Some optimizations can be done maintaining the assumption that the motor perfectly performs the reference task. Some examples are the minimization of the overall cost of electronic drive, motor and transmission, their overall weight or, somehow, the volume of motor and transmission. Another example is the minimization of the energy dissipated in a cycle, taking also into account the power waste in the transmission, by assuming that inside the motor there is linearity between torque and current and that the power waste is only due to the Joule effect. It is of course possible to resort to a multi-objective optimization by means of a suitable linear combination of single-objective functions.

Other optimizations, such as those concerning the control performance, are more demanding, because they require at least the coupling of a complex model of the motor and the transmission, and also of the controllers, with a model of the rest of the machine.

4. Graphical Solution: Torque Peak Curve

Instead of an automated procedure, the designer often desires to resort to a graphical representation, which allows him a concise comparison among different solutions. In this case, it is convenient to fix a given transmission and to use a diagram in which the corresponding torque peak curve $M_{m,max}(J_M)$ is drawn together with the motor representative points, as explained below.

According to Equation (16), for each value of J_M, the maximum value $M_{m,max}$ assumed by $|M_m(t;\ J_M)|$ over time must be found. The curve $M_{m,max}(J_M)$ thus obtained is called *torque peak curve* and is denoted by p. The torque peak curve p lies in the first quadrant of the $J_M - M_{m,max}$ plane and can be drawn directly by means of Equation (16), in which J_M is a parameter that increases from zero to a suitable maximum value. Here another way is proposed that allows the designer to find its analytical expression and to explain its shape. As will be explained later, it is continuous, consists of a sequence of segments and shows only one minimum point.

4.1. From Points $\left(\alpha_l, \hat{M}'_l\right)$ to Points $\left(\alpha_l, \hat{M}'^*_l\right)$

In order to draw the torque peak curve p, some of the conclusions explained in [21] are reported here.

At a given time instant t, in the $J_M - |M_m|$ plane, Equation (15) corresponds to a curve lying in the first quadrant. This curve depends on the $\left[\alpha_l(t),\ \hat{M}'_l(t)\right]$ pair, which changes as time increases.

In the $\alpha_l - \hat{M}'_l$ plane instead of considering the original points $\left(\alpha_l,\ \hat{M}'_l\right)$ as time t varies, it is convenient to refer to a new set of points $S^* \equiv \left(\alpha^*_l,\ \hat{M}'^*_l\right)$ that derive from the original ones according with the following rules:

- If $\hat{M}'_l$ and α_l have the same sign, positive or negative, or are both null, one set of points S^* lying in the first quadrant of the $\alpha_l - \hat{M}'_l$ plane must be taken into consideration; they have abscissa equal to $|\alpha_l|$ and ordinate equal to $\left|\hat{M}'_l\right|$. In the $J_M - |M_m|$ plane the corresponding half-line s^*_l lies in the first quadrant (Figure 5) and contributes to the ascending branch of the torque peak curve.
- If $\hat{M}'_l$ and α_l have opposite sign, then two sets of points, symmetrical with respect to the origin, must be taken into account:
  - (1) The first set lies in the second quadrant of the $\alpha_l - \hat{M}'_l$ plane; these points have abscissa equal to $-|\alpha_l|$ and ordinate equal to $\left|\hat{M}'_l\right|$. In the $J_M - |M_m|$ plane the

corresponding segment s^*_{II} lies in the first quadrant (Figure 5) and can only contribute to the descending branch of the torque peak curve.

(2) The second set lies in the fourth quadrant of the $\alpha_l - \hat{M}'_l$ plane; these points have abscissa equal to $|\alpha_l|$ and ordinate equal to $-|\hat{M}'_l|$. In the $J_M - |M_m|$ plane the corresponding segment s^*_{IV} lies in the first quadrant (Figure 5) and can only contribute to the ascending branch of the torque peak curve.

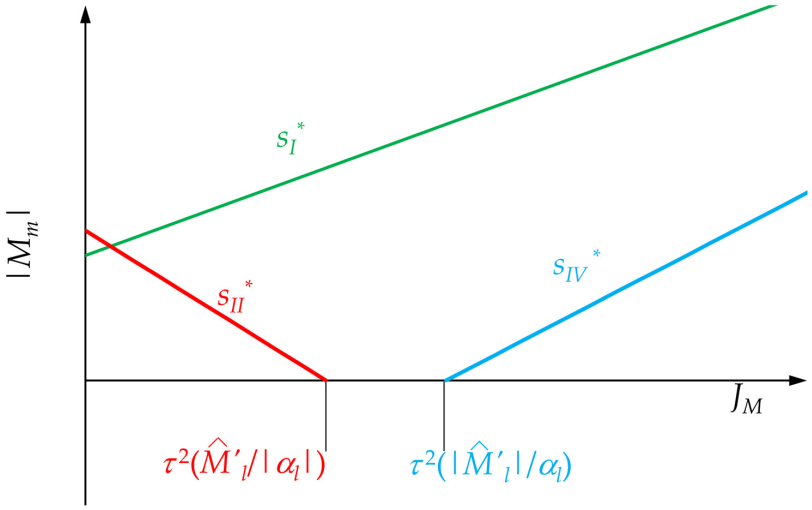

Figure 5. Examples of curves s^*_I, s^*_{II} and s^*_{IV} corresponding to points S^* lying in the first, second and fourth quadrant of the $\alpha_l - \hat{M}'_l$ plane, respectively.

4.2. Points $(\alpha^*_l, \hat{M}'^*_l)$ That Contribute to the Torque Peak Curve

Nevertheless, not all the points S^* lying in the first, second and fourth quadrant of the $\alpha_l - \hat{M}'_l$ plane contribute to the torque peak curve p. Only few points affect this curve. Indicating their number with n, they are denoted by K^*_j, with $j = 1, 2, \ldots, n$. They are the vertices of a simple polygonal chain (Figure 6), denoted by k, with the following features:

- The concavity of k is always directed towards the same region of the $\alpha_l - \hat{M}'_l$ plane, i.e., downwards and leftwards.
- All the other points S^*, distinct from the vertices K^*_j, lie inside this region.
- The first side of k is a horizontal half-line, the last side is a vertical half-line.

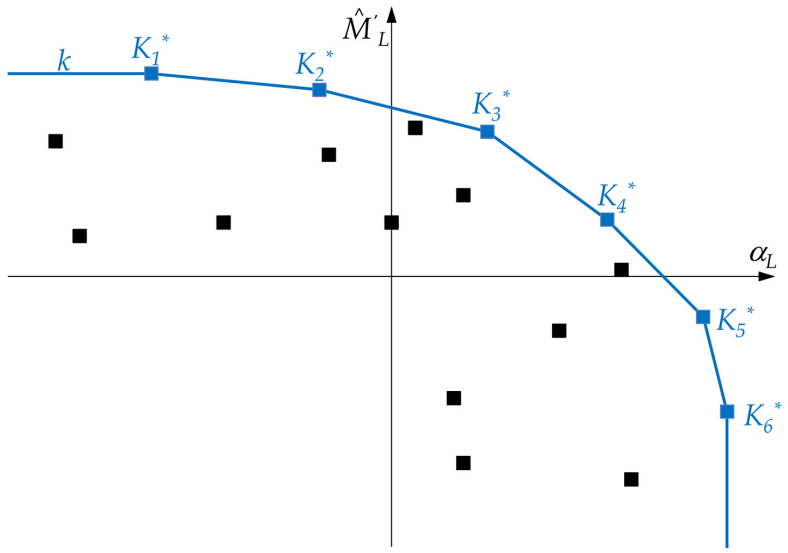

Figure 6. Polygonal chain k and vertices K^*_j that contribute to the torque peak curve p.

All the vertices K_j^* affecting the torque peak curve p can be found by means of a simple software program.

4.3. Shape of the Torque Peak Curve

It is now possible to find the equation of the torque peak curve. In the J_M-$M_{m,max}$ plane, Figure 7 shows the different straight-lines k_j^* corresponding to the points K_j^* shown in Figure 6, and the resulting torque peak curve p. The equation of the generic segment corresponding to the vertex K_j^* is

$$M_{m,max} = \frac{\alpha_{l,K_j^*}}{\tau} J_M + \tau \hat{M}'_{l,K_j^*} \tag{18}$$

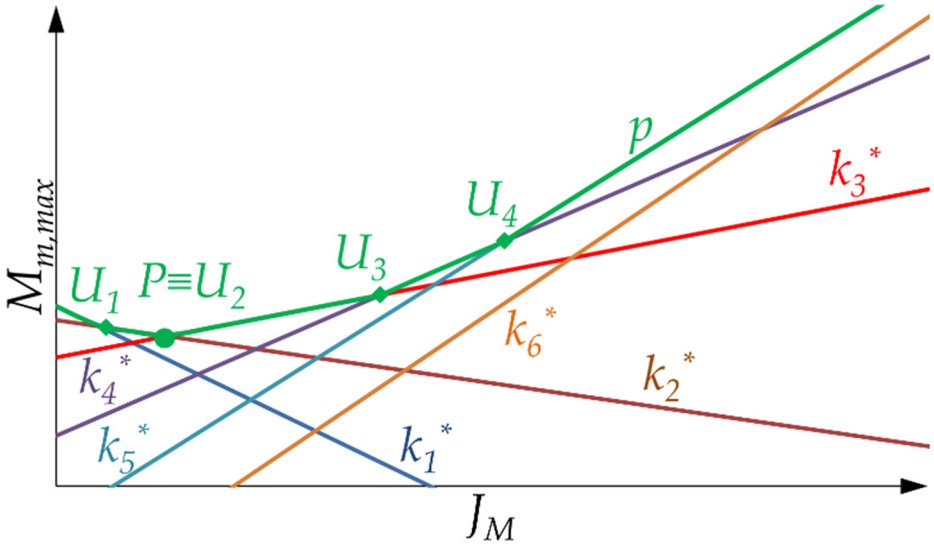

Figure 7. The straight lines k_j^* corresponding to points K_j^* in Figure 6 and the torque peak curve p.

The abscissa of the intersection U_j with the next branch is

$$J_M|_{U_j} = \tau^2 \frac{\hat{M}'_{l,K_{j+1}^*} - \hat{M}'_{l,K_j^*}}{\alpha_{l,K_j^*} - \alpha_{l,K_{j+1}^*}} \tag{19}$$

while its ordinate is

$$M_{m,max}|_{U_j} = \tau \frac{\hat{M}'_{l,K_{j+1}^*} \alpha_{l,K_j^*} - \hat{M}'_{l,K_j^*} \alpha_{l,K_{j+1}^*}}{\alpha_{l,K_j^*} - \alpha_{l,K_{j+1}^*}} \tag{20}$$

Equations (18)–(20), whose parameters only depend on the reference task and the given transmission, allow the automatic writing of the equation of the global torque peak curve p.

This is a simple polygonal chain in the first quadrant of the J_M -$M_{m,max}$ plane. It is made up of consecutive segments, corresponding to the consecutive points K_j^*. Only its last element is a half-line. These segments belong to straight lines having the following features:

(1) Their slope is negative or positive according to the sign of α_{l,K_j^*}, i.e., according to the position of vertex K_j^* either in the second quadrant of the $\alpha_l - \hat{M}'_l$ plane or in the first and fourth.
(2) Their intersection with the ordinate axis is positive or negative according to the sign of $\hat{M}'_{l,K_j^*}$, i.e., according to the position of vertex K_j^* either in the first and second quadrants of the $\alpha_l - \hat{M}'_l$ plane or in the fourth.
(3) Going from one point K_j^* to the next one, the segment slope increases.

The first segment of the torque peak curve p can have either negative or positive slope; the last segment always has a positive slope. Therefore, generally, the torque peak curve is made up of a sequence of descending segments followed by a sequence of ascending segments: between the two sequences, there is a minimum point P. Obviously, if there is only a sequence of ascending segments, the abscissa of the minimum point P is null.

4.4. Drive System Representative Points

In the same diagram where the torque peak curve p is plotted, each of the drive systems is represented by a point: the generic j-th drive system corresponds to a point D_j (Figure 8) whose ordinate is its limit torque $M_{M,dyn}$ and whose abscissa is the moment of inertia J_M of the motor.

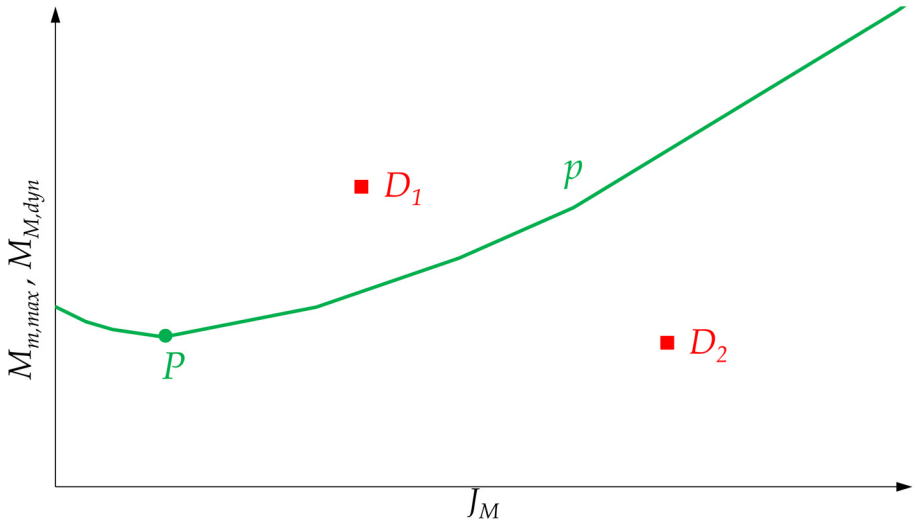

Figure 8. Torque peak curve p and drive system representative points D_j.

Considering the first of inequalities (17), there are two cases:

(1) If the drive system representative point lies above the torque peak curve p, for example D_1, the motor, coupled with the given speed reducer, is able to drive the load according to the reference task and is admissible.
(2) Conversely, drive systems whose representative points lie below curve p, for example D_2, must be excluded for the given transmission.

In short, considering an admissible transmission and keeping in mind inequalities (17), a drive system can be coupled with this speed reducer from the point of view of its dynamic operating range if these simultaneous conditions are met:

– Its representative point does not lie below the torque peak curve p in the diagram in Figure 8.
– Its maximum achievable speed satisfies the second of inequalities (17).

Figure 9 shows the flowchart of the graphical procedure. Until the analysis of admissibility of the given transmission, it coincides with the flowchart in Figure 4.

Both the torque peak curve and the rms torque curve in [25] show a minimum point, even though in general the abscissas of these points are different. In trend line, drive systems whose representative points lie above these curves and near the minimum points are admissible for the given transmission and characterized by a smaller cost and size. However, also the cost and size of the transmission must be kept into account.

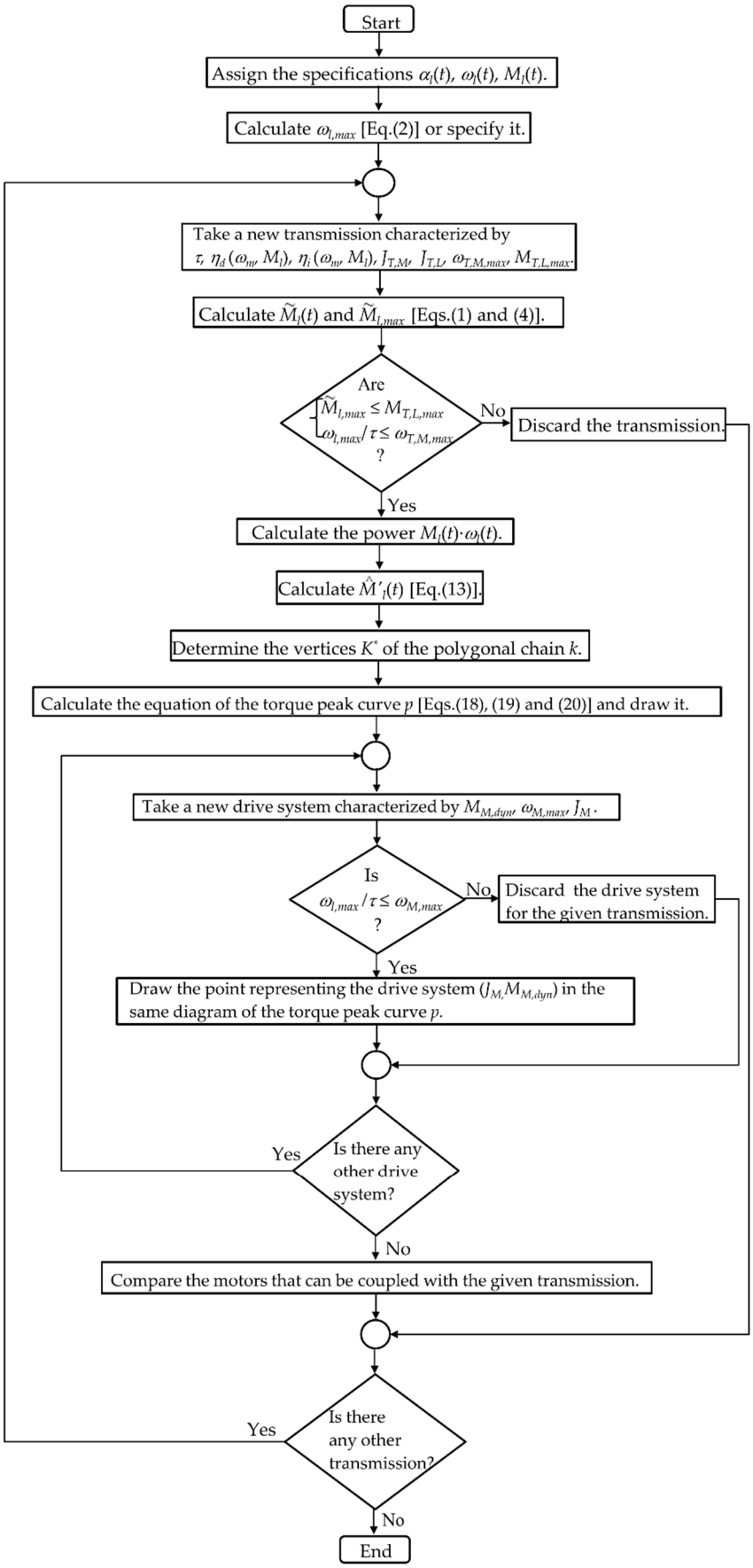

Figure 9. Flowchart of the graphical procedure to find all the drive systems that can be coupled with an admissible transmission.

This procedure also allows the designer to identify on which elements of the specifications (and the transmission parameters) the shape of the torque peak curve depends. Sometimes, the specifications are not rigid, and the designer can slightly modify them in view of other benefits, for example, the choice of a motor otherwise to be discarded or, for an interesting admissible drive system–transmission couple, the decrease of the period of the reference task. However, the effects of these modifications must also be examined with reference to the thermal problem of the motor.

5. A Case Study

The same flying machine for sealing and cutting already examined in [25] from the point of view of the motor thermal problem is here analyzed from the point of view of the torque peak of the motor. The reference task is periodic with a period of 0.08 s and is characterized by a global rotation of the load of $2\pi/3$ rad. The acceleration and speed of the load together with the global torque M_l can be found in [25] as functions of time.

The same transmission considered in [25] is now taken into account. Its characteristics are summarized in Table 1. The direct and inverse efficiency do not depend on speed.

Table 1. Characteristics of the transmission considered.

t	η_d	η_i	$\omega_{T,M,max}$	$M_{T,L,max}$	$J_{T,M}$	$J_{T,L}$
			(rad/s)	**(Nm)**	**(kg m^2)**	**(kg m^2)**
0.125	0.94	0.92	314.16	32.0	$0.028 \cdot 10^{-4}$	negligible

In [25], this transmission was already found admissible.

The same four drive systems D_1, D_2, D_3 and D_4 considered in [25] are candidate to move the load. Their dynamic operating range is rectangular, and their characteristic parameters are shown in Table 2. As already shown in [25], all the four motors meet the speed inequality (17).

Table 2. Characteristics of the drive systems candidate to move the load.

Drive System	J_M	$M_{M,dyn}$	$\omega_{M,max}$
	(kg m^2)	**(Nm)**	**(rad/s)**
D_1	$7.25 \cdot 10^{-5}$	2.9	314.16
D_2	$1.25 \cdot 10^{-4}$	5.7	314.16
D_3	$2.50 \cdot 10^{-4}$	11.4	314.16
D_4	$3.50 \cdot 10^{-4}$	16.2	314.16

During the period, the power flow through the transmission shows an alternation from motor to load (when $\widetilde{M}_l\omega_l$ is positive) and from load to motor (when $\widetilde{M}_l\omega_l$ is negative).

To draw the torque peak curve p requires the determination of the vertices K_j^* in the $\alpha_l - \hat{M}_l'$ plane. In Figure 10, the brown curves are the locus of a point S^*. The polygonal chain k is made up of a horizontal and a vertical half-line, and only vertex K_1^* gives contribution to the torque peak curve p.

In Figure 11, the representative points D_1, D_2, D_3 and D_4 of the four drive systems taken into consideration are drawn, together with the torque peak curve p. Since points D_2, D_3 and D_4 lie above curve p, only these motors can be coupled with the given transmission from the point of view of the limit torque $M_{M,dyn}$ of the dynamic operating range.

Since only drive systems D_3 and D_4 gave a positive result from the point of view of the motor thermal problem [25], finally, these are the only motors that, coupled with the given transmission, are able to perform the reference task from all the points of view.

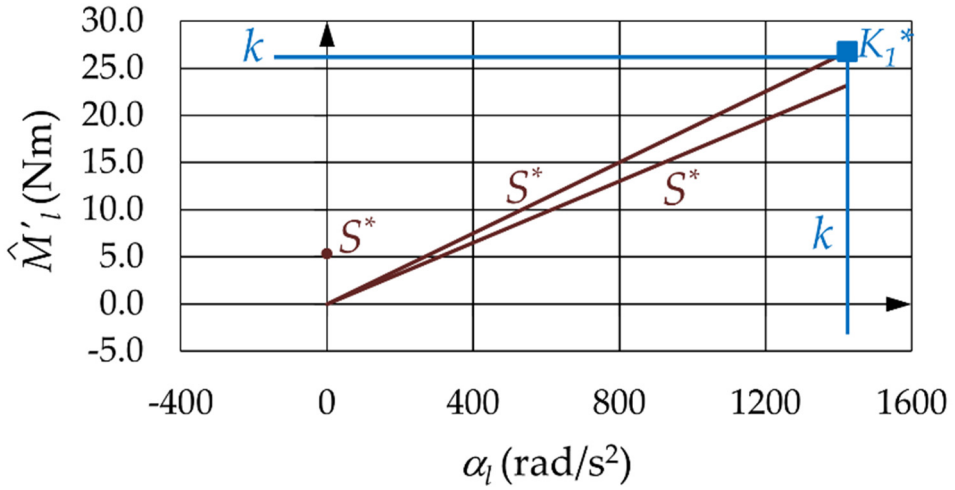

Figure 10. Points S^*, vertex K_1^* and polygonal chain k in the $\alpha_l - \hat{M}'_l$ plane.

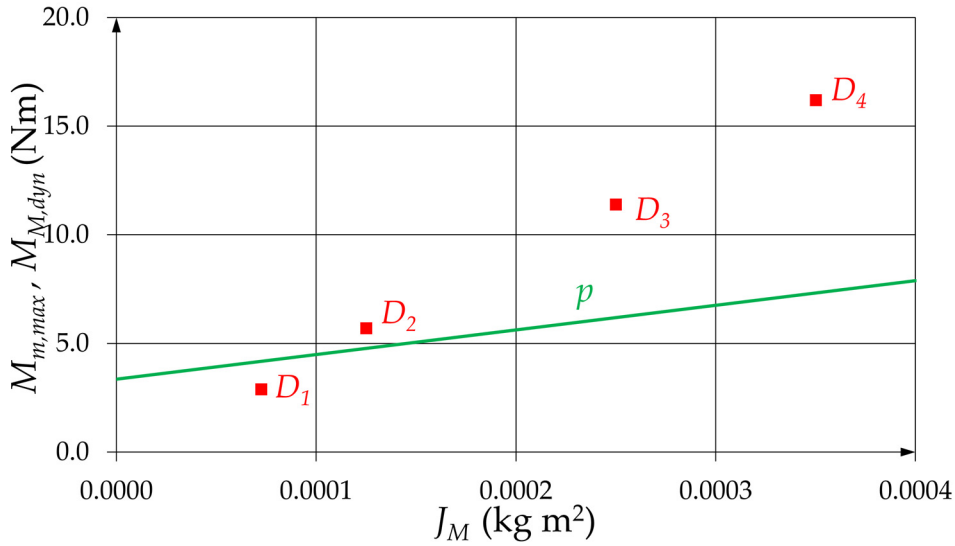

Figure 11. Torque peak curve p and representative points of the drive systems.

6. Non-Rectangular Dynamic Operating Range

The diagram in Figure 8 can also be suitably modified to solve the torque peak problem for many drive systems whose limit torque of the dynamic operating range does depend on motor speed.

Obviously, a motor must first meet the second of inequalities (17).

If the dynamic operating range of the drive system is non-rectangular, its limit curve shows two characteristic points (Figure 1): N_1, whose coordinates are $\omega_{M,1}$ and $M_{M,dyn,1}$, and N_2, whose coordinates are $\omega_{M,max}$ and $M_{M,dyn,2}$. Torque $M_{M,dyn}$ is constant and equal to $M_{M,dyn,1}$ when the speed is lesser than $\omega_{M,1}$, whereas, on the right of N_1, $M_{M,dyn}$ decreases as far as speed $\omega_{M,max}$.

When drawing a diagram like that shown in Figure 8, the torque peak curve does not change, whereas a drive system is no longer characterized by a single point D; conversely, in correspondence to the same abscissa J_M of the motor, there is a vertical segment $D_{N_1}D_{N_2}$ (Figure 12): the ordinate of the highest extreme D_{N_1} is equal to $M_{M,dyn,1}$ and that of the lowest extreme D_{N_2} is equal to $M_{M,dyn,2}$.

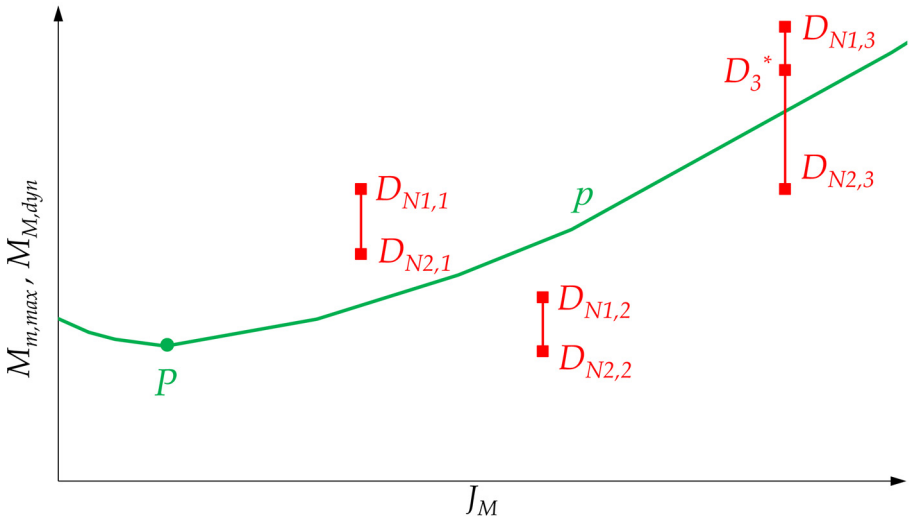

Figure 12. Torque peak curve p and representative segments of the drive systems.

Considering the position of this segment with respect to the torque peak curve p, it is possible to find some sufficient conditions. There are three cases:

(1) If D_{N_2} lies above curve p (drive system D_1), the entire segment $D_{N_1}D_{N_2}$ lies above this curve and the motor can certainly be adopted with the given transmission. In fact, even a motor with a rectangular operating range whose limit torque is equal to $M_{M,dyn,2}$ can be adopted.

(2) If D_{N_1} lies below curve p (drive system D_2), the entire segment $D_{N_1}D_{N_2}$ lies below this curve, and the motor must be excluded for the transmission into consideration. In fact, even a motor with a rectangular operating range whose limit torque is equal to $M_{M,dyn,1}$ must be excluded.

(3) If D_{N_1} lies above and D_{N_2} lies below curve p (drive system D3), three cases can be distinguished:

   (a) If $\omega_{m,max}$ is not greater than $\omega_{M,1}$, then the motor can certainly be coupled with the given transmission because this case is similar to that of a rectangular dynamic operating range whose limit torque is equal to $M_{M,dyn,1}$.

   (b) If $\omega_{m,max}$ is greater than $\omega_{M,1}$ and $M_{M,dyn}(\omega_{m,max})$ is greater than $M_{m,max}(J_M)$ (point $D_3{}^*$ for drive system D_3), then motor and transmission can be coupled because this case is similar to that of a rectangular dynamic operating range with a limit torque equal to $M_{M,dyn}(\omega_{m,max})$.

   (c) Otherwise [23], based on this diagram, it is not possible to determine whether the motor is able to drive the load. In this case, it is necessary to go on with a more detailed analysis of the drive system–transmission couple. More precisely, for the drive system in consideration the analytical equation of the limit curve $M_{M,dyn}(\omega_m)$ of the dynamic operating range must be found, by means of either physical equations or mathematical interpolation of the graphic curve. At each time instant t, the values $M_m(t)$ of the motor torque and $\omega_m(t)$ of its speed are known by means of Equations (14) and (3), respectively. As t increases from zero to the period, in the first quadrant of the characteristic plane $\omega_m - M_m$ of the motor, $|M_m(t)|$ must be not greater than $M_{M,dyn}[\omega_m(t)]$, i.e., the locus of a point whose coordinates are $|\omega_m(t)|$ and $|M_m(t)|$, with t as a parameter, must lie inside the dynamic operating range of the drive system. The check can be either automated or graphic.

7. Effect of a Viscous Torque inside the Motor

This section shows how the proposed procedure can be modified when inside the motor, there is a considerable viscous torque due to the iron losses. The treatment is similar

when, instead of a viscous torque, there are other resistant torques that are known functions of speed. The equations are those of a DC motor. Linearity is assumed between the ideal torque $M_{m,i}$ of the motor and current i, according to the torque constant K_T:

$$M_{m,i} = K_T i. \tag{21}$$

Taking into account the iron losses, the available torque M_m to accelerate the motor itself and to move transmission and load is given by

$$M_m = M_{m,i} - b\omega_m = K_T i - b\omega_m, \tag{22}$$

where M_m, because of the equilibrium equation, is given by Equation (14).

The motor current assumes the value:

$$i = \frac{M_m + b\omega_m}{K_T}. \tag{23}$$

Both the thermal problem of the motor and the torque peak problem of the drive system will now be analyzed.

7.1. Thermal Problem of the Motor

From the point of view of the power losses inside the motor, there are now two differences:

(1) As i changes, the Joule losses in the winding resistances change too.
(2) The iron losses are added to the copper losses.

The dissipated power is given by

$$W_d = Ri^2 + b\omega_m^2, \tag{24}$$

where R denotes an appropriate resistance of the windings, and the second term refers to the effect of the viscous torque (iron losses).

According to Equation (23), the dissipated power assumes the value

$$W_d = R\left(\frac{M_m + b\omega_m}{K_T}\right)^2 + b\omega_m^2. \tag{25}$$

If the thermal behavior of the motor is governed by a first order differential equation and the periodic reference task has a period T much lesser than the thermal time constant of the motor, in this differential equation on the right-hand side, there is a constant known term that is the average dissipated power in the period. This is due to the fact that the variations of the dissipated power in the period are filtered with respect to the average value, denoted by $\overline{W}_d$, which, according to Equation (25), is given by

$$\begin{aligned} \overline{W}_d &= \tfrac{R}{K_T^2}\tfrac{1}{T}\int_0^T M_m^2 dt + b^2\tfrac{R}{K_T^2}\tfrac{1}{T}\int_0^T \omega_m^2 dt + 2b\tfrac{R}{K_T^2}\tfrac{1}{T}\int_0^T M_m\omega_m dt + b\tfrac{1}{T}\int_0^T \omega_m^2 dt \\ &= \tfrac{R}{K_T^2}M_{m,rms}^2 + \left(b^2\tfrac{R}{K_T^2} + b\right)\omega_{m,rms}^2 + 2b\tfrac{R}{K_T^2}\tfrac{1}{T}\int_0^T M_m\omega_m dt. \end{aligned} \tag{26}$$

Keeping in mind Equation (14), in the last term, the integral can be written as

$$\begin{aligned} &\int_0^T M_m\omega_m dt = \int_0^T \left[\tfrac{J_M}{\tau}\alpha_l(t) + \tau\hat{M}_l'(t)\right]\tfrac{\omega_l(t)}{\tau}dt = \int_0^T \tfrac{J_M}{\tau^2}\alpha_l(t)\omega_l(t)\,dt + \int_0^T \hat{M}_l'(t)\omega_l(t)\,dt \\ &= \tfrac{1}{2}\tfrac{J_M}{\tau^2}\int_{\omega_l(0)}^{\omega_l(T)} d\omega_l^2 + \int_0^T \hat{M}_l'(t)\omega_l(t)\,dt. \end{aligned} \tag{27}$$

The first term on the right-hand side is equal to zero because at the end of the period the speed assumes its initial value. The second term can be calculated and is denoted by $\overline{\hat{W}}_l' \cdot T$.

Hence, the dissipated power assumes the expression

$$\overline{W}_d = \frac{R}{K_T^2} M_{m,rms}^2 + \left(b^2 \frac{R}{K_T^2} + b \right) \omega_{m,rms}^2 + 2b \frac{R}{K_T^2} \overline{\hat{W}}_l'. \tag{28}$$

If $M_{M,S}$ is the stall torque, in mechanical and thermal steady state conditions, at the limit temperature that the motor can reach, the corresponding dissipated power at the different speeds is always given by

$$W_{d,S1} = \frac{R}{K_T^2} M_{M,S}^2. \tag{29}$$

The subscript S1 is due to the fact that this is the dissipated power along the limit curve of the continuous duty operating range S1.

In order to avoid the over-heating of the motor, the average dissipated power in the period must be lesser than this value:

$$\overline{W}_d \leq W_{d,S1} = \frac{R}{K_T^2} M_{M,S}^2. \tag{30}$$

The result is

$$\frac{R}{K_T^2} M_{m,rms}^2 + \left(b^2 \frac{R}{K_T^2} + b \right) \omega_{m,rms}^2 + 2b \frac{R}{K_T^2} \overline{\hat{W}}_l' \leq \frac{R}{K_T^2} M_{M,S}^2, \tag{31}$$

and after dividing all terms by R/K_T^2,

$$M_{m,rms}^2 + \left(b^2 + b \frac{K_T^2}{R} \right) \omega_{m,rms}^2 + 2b \overline{\hat{W}}_l' \leq M_{M,S}^2. \tag{32}$$

Isolating $M_{m,rms}$ on the left-hand side, the following inequality is obtained

$$M_{m,rms} \leq \sqrt{M_{M,S}^2 - \left(b^2 + b \frac{K_T^2}{R} \right) \frac{\omega_{l,rms}^2}{\tau^2} - 2b \overline{\hat{W}}_l'}. \tag{33}$$

According to [25], $M_{m,rms}$ is a known function of J_M, called rms torque curve r, given by

$$M_{m,rms} = \sqrt{\frac{J_M^2}{\tau^2} \alpha_{l,rms}^2 + 2 J_M \hat{G}_l' + \tau^2 \hat{M}_{l,rms}'^2}, \tag{34}$$

with

$$\hat{G}_l' = \frac{1}{T} \int_0^T \hat{M}_l'(t)\, \alpha_l(t) dt. \tag{35}$$

The same procedure shown in [25] can now be used, with the same rms torque curve r, which is a hyperbola in the first quadrant of the $J_M - M_{m,rms}$ plane that does not depend on the drive system (Figure 13). Nevertheless, the representation of the motor is different. In fact, according to Equation (32), an *equivalent* motor is represented by a point whose

abscissa is still its moment of inertia J_M, whereas its ordinate is now the equivalent torque $M_{M,eq}$ given by

$$M_{M,eq} = \sqrt{M_{M,S}^2 - \left(b^2 + b\frac{K_T^2}{R}\right)\frac{\omega_{l,rms}^2}{\tau^2} - 2b\overline{\hat{W}}_l'}, \tag{36}$$

which depends not only on the motor but also on the transmission and the reference task.

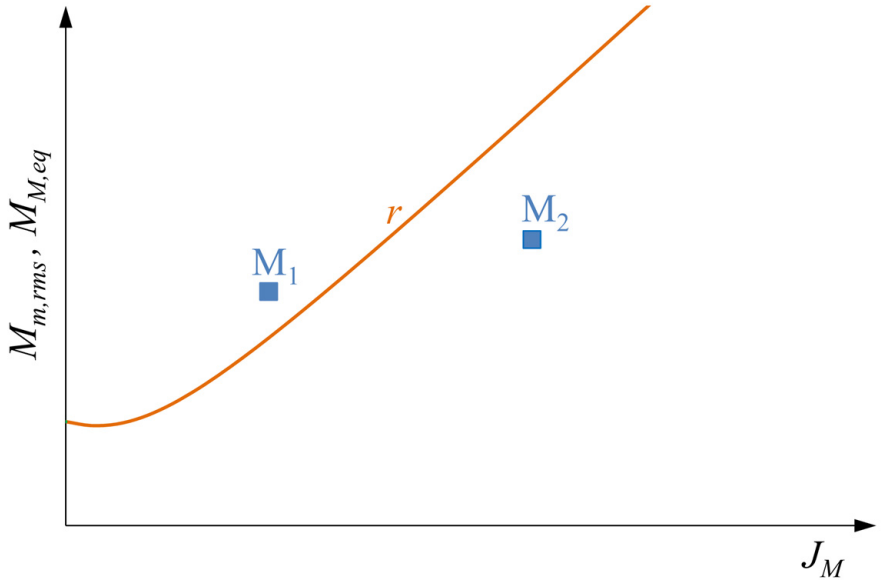

Figure 13. Rms torque curve r and representative points M_j of the equivalent motors.

If the representative point of the equivalent motor lies above the rms torque curve r (motor M_1), the drive system can be coupled with the given transmission in order to perform the reference task (from the point of view of the thermal problem of the motor). On the contrary, if it lies below (motor M_2), it must be definitively excluded.

If, instead of a graphical representation, the designer decides to use an automated procedure, Equations (33) and (34) allow him to do it easily.

7.2. Torque Peak Problem of the Drive System

As regards the torque peak problem, the available motor torque is given by Equation (22), but the limit torque $M_{m,dyn}$ of the dynamic range corresponds to the ideal motor torque $M_{m,i}$ given by Equation (21) when the current reaches the maximum value i_{max} allowed by the electronic driver:

$$M_{m,dyn} = K_T i_{max}. \tag{37}$$

According to Equation (22), the ideal torque of the motor is equal to

$$M_{m,i}(t) = M_m(t) + b\omega_m(t). \tag{38}$$

In order to avoid the torque peak problem, the following inequality must be respected

$$\left|M_{m,i}(t)\right| = \left|M_m(t) + b\omega_m(t)\right| \leq M_{m,dyn}. \tag{39}$$

Keeping in mind Equation (14), the result is

$$\left|\frac{J_M}{\tau}\alpha_l(t) + \tau\hat{M}_l'(t) + b\frac{\omega_l(t)}{\tau}\right| \leq M_{m,dyn}. \tag{40}$$

This inequality is like the first of inequalities (17), by replacing the torque $\hat{M}_l''(t)$, given by

$$\hat{M}_l''(t) = \hat{M}_l'(t) + b\frac{\omega_l(t)}{\tau^2}, \tag{41}$$

instead of $\hat{M}_l'(t)$ in the expression of $M_{m,max}$:

$$\max_t \left| \frac{J_M}{\tau}\alpha_l(t) + \tau\hat{M}_l''(t) \right|.$$

The difference with respect to the first of inequalities (17) is that the right-hand side also depends on the motor, through the parameter b.

Hence, the corresponding torque peak curve p now depends not only on the reference task and the transmission but also on the motor. Nevertheless, it obviously has the same general characteristics of a torque peak curve, already seen in Section 4. In particular, this curve shows a possible descending branch, a minimum point and an ascending branch. Obviously, by changing b as a parameter, the corresponding curves are different, for example, as regards the position of the minimum point (Figure 14).

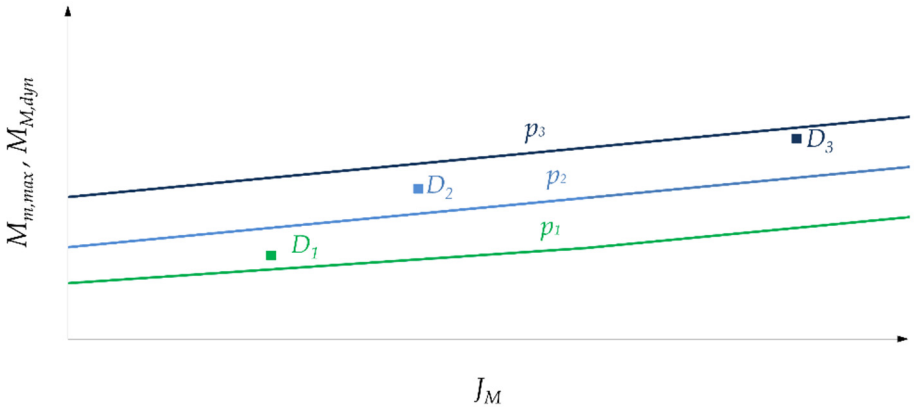

Figure 14. Torque peak curves p_i and representative points D_i of the drive systems.

Hence, in the first quadrant of the plane $J_M - M_{m,max}$, a family of curves, with b as a parameter, can be drawn. On the contrary, each drive system is still represented by the same point as in Section 4, whose abscissa is its moment of inertia J_M and ordinate is $M_{M,dyn}$. Nevertheless, this point must be labeled by means of the corresponding value of b, in order to compare it with the corresponding torque peak curve.

If the representative point of the drive system lies above the corresponding curve (drive systems D_1 and D_2), this drive system can be coupled with the given transmission in order to perform the reference task (from the point of view of the torque peak problem). Otherwise (drive system D_3), it must be definitively excluded.

If instead the designer decides to proceed with an automated calculation, Equations (42) and (17) permit him to do it easily.

8. Conclusions

This work deals with the admissible drive system-transmission couples from the point of view of the torque peak of the motor, i.e., those couples that are able to perform the reference task from this perspective. It proposes a method by which all these couples are found *from the outset*. This means that transmission ratio, reducer efficiencies and their dependency on speed and torque, inertia of the speed reducer, limits of speed and torque of the reducer, motor inertia, limits of speed and torque of the drive system, i.e., all the elements playing a role in the choice, are taken into account in a complete and effective way. Furthermore, the most general case, in which during the cycle there is alternation between direct and inverse power flow through the transmission, is considered. This method allows the designer to avoid any further check.

Starting from the common case of a rectangular dynamic operating range of the drive system, the rationale of the proposed method is to take the candidate transmissions from the catalogs one by one, so that all their parameters are known from the outset.

After excluding the not admissible transmissions, whose limits of speed and torque are not compatible with the reference task, for each of the other reducers, all candidate drive-systems are examined one at a time. For each motor, its torque peak during the reference task is determined by means of an equation that takes into account all the most significant factors on which it depends. Its comparison with the limit torque of the dynamic operating range allows an automatic check to ascertain if the drive system under analysis can be coupled with the transmission taken into consideration.

In addition to an automated procedure, a graphical representation provides the designer a concise view of all the drive systems that can be coupled with a given admissible transmission. More in detail, a *torque peak curve* can be drawn as a function of the unknown moment of inertia of the motor; this curve is only related to the reference task and to the transmission parameters. In this diagram, each drive system is represented by a point that is compared with the *torque peak curve* in order to accept or exclude the motor. This graphical interpretation must be repeated for each admissible transmission.

Furthermore, for many drive systems whose dynamic operating range is non-rectangular, this work explains how to apply a similar procedure. For the remaining drive systems, a more complex method is explained.

Finally, the paper shows how the proposed method can be applied to motors that present an internal viscous torque due to the iron losses (also with reference to the thermal problem of the motor).

Therefore, this work, together with paper [25], which similarly deals with the motor thermal problem, is an interesting instrument to determine from the outset the admissible drive system-transmission couples for a given reference task. An optimization phase must follow this feasibility stage.

In a future work, the authors will study the non-linearities of the motor that influence its choice.

Author Contributions: Formal analysis and methodology, F.C. and G.C.; conceptualization and writing—original draft, G.C. Both authors have read and agreed to the published version of the manuscript.

Funding: This research received no external funding.

Data Availability Statement: The data presented in this study are openly available in ScienceDirect at https://doi.org/10.1016/j.mechatronics.2016.09.004 (accessed on 2 August 2021).

Conflicts of Interest: The authors declare no conflict of interest.

Nomenclature

Symbol	Unit	Description
b	Nm s/rad	viscous constant of a DC motor
i	A	current in a DC motor
i_{max}	A	maximum current in a DC motor allowed by the electronic driver
J_M	kg m^2	moment of inertia of the motor
$J_{T,L}$	kg m^2	moment of inertia of the transmission on load side
$J_{T,M}$	kg m^2	moment of inertia of the transmission on motor side
K_T	Nm/A	torque constant of a DC motor
M_l	Nm	load torque
$\widetilde{M}_l$	Nm	reducer torque on load side
$\widetilde{M}_{l,max}$	Nm	maximum value of $\left\lvert \widetilde{M}_l(t) \right\rvert$

$\widetilde{M}'_l$	Nm	reducer torque taking into account the transmission efficiency
$\hat{M}'_l$	Nm	torque taking into consideration the transmission efficiency and the transmission inertia on load and motor side
$\hat{M}'_{l,rms}$	Nm	rms value of $\hat{M}'_l$ during the reference task
$\hat{M}'^{*}_l$	Nm	a suitable transformation of $\hat{M}'_l$
M_m	Nm	current motor torque
$M_{m,i}$	Nm	ideal torque of a DC motor
$M_{M,dyn}$	Nm	limit torque of the dynamic operating range of the drive system
$M_{M,dyn,1}$	Nm	limit torque of the dynamic operating range of the drive system up to speed $\omega_{M,1}$
$M_{M,dyn,2}$	Nm	limit torque of the dynamic operating range of the drive system at speed $\omega_{M,max}$
$M_{M,eq}$	Nm	a suitable equivalent torque of the motor
$M_{M,S}$	Nm	stall torque of the motor at its limit temperature
$M_{T,L,max}$	Nm	maximum torque that the transmission can bear on load side
R	Ω	resistance of the windings
t	s	time
T	s	period of the cyclic reference task
$W_{d,S1}$	W	dissipated power in the motor in steady state conditions at its limit temperature
W_d	W	dissipated power in the motor
$\overline{W}_d$	W	average dissipated power during the reference task
$\overline{\hat{W}'_l}$	W	average power associated with $\hat{M}'_l$ during the reference task
α_l	rad/s^2	load angular acceleration
$\alpha_l{}^*$	rad/s^2	a suitable transformation of α_l
$\alpha_{l,rms}$	rad/s^2	rms angular acceleration of the load during the reference task
η_d		direct efficiency of the transmission
η_i		inverse efficiency of the transmission
τ		transmission ratio
ω_l	rad/s	load angular speed
$\omega_{l,max}$	rad/s	maximum value of $\lvert\omega_l(t)\rvert$ during the reference task
$\omega_{l,rms}$	rad/s	rms value of the load speed during the reference task
ω_m	rad/s	motor angular speed
$\omega_{m,max}$	rad/s	maximum value of $\lvert\omega_m(t)\rvert$ during the reference task
$\omega_{M,max}$	rad/s	maximum speed reachable by the motor
$\omega_{M,1}$	rad/s	motor speed beyond which $M_{M,dyn}$ is no more constant
$\omega_{T,M,max}$	rad/s	maximum speed of the transmission on motor side

References

1. Roos, F.; Johansson, H.; Wikander, J. Optimal selection of motor and gearhead in mechatronic application. *Mechatronics* **2006**, *16*, 63–72. [CrossRef]
2. Pettersson, M.; Ölvander, J. Drive train optimization for industrial robots. *IEEE Trans. Robot.* **2009**, *25*, 1419–1424. [CrossRef]
3. Zhou, L.; Bai, S.; Hansen, M.R. Design optimization on the drive train of a light-weight robotic arm. *Mechatronics* **2011**, *21*, 560–569. [CrossRef]
4. Ge, L.; Chen, J.; Li, R.; Liang, P. Optimization design of drive system for industrial robots based on dynamic performance. *Ind. Robot Int. J.* **2017**, *44*, 765–775. [CrossRef]
5. Padilla-Garcia, E.A.; Rodriguez-Angeles, A.; Reéndiz, J.R.; Cruz-Villar, C.A. Concurrent optimization for the selection and control of ac servomotors on the powertrain of industrial robots. *IEEE Access* **2018**, *6*, 27923–27938. [CrossRef]
6. Nasiri, R.; Khoramshahi, M.; Shushtari, M.; Ahmadabadi, M.N. Adaptation in variable parallel compliance: Towards energy efficiency in cyclic tasks. *IEEE-ASME Trans. Mechatron.* **2017**, *22*, 1059–1070. [CrossRef]
7. Verstraten, T.; Beckerle, P.; Furnémont, R.; Mathijssen, G.; Vanderborght, B.; Lefeber, D. Series and parallel elastic actuation: Impact of natural dynamics on power and energy consumption. *Mech. Mach. Theory* **2016**, *102*, 232–246. [CrossRef]
8. Haddadin, S.; Mansfeld, N.; Albu-Schäffer, A. Rigid vs. elastic actuation: Requirements & performance. In Proceedings of the IEEE/RSJ International Conference on Intelligent Robots and Systems, Vilamoura, Algarve, Portugal, 7–12 October 2012; pp. 5097–5104.
9. Saerens, E.; Crispel, S.; García, P.L.; Verstraten, T.; Ducastel, V.; Vanderborght, B.; Lefeber, D. Scaling laws for robotic transmissions. *Mech. Mach. Theory* **2019**, *140*, 601–621. [CrossRef]
10. Saerens, E.; Furnémont, R.; Verstraten, T.; García, P.L.; Crispel, S.; Ducastel, V.; Vanderborght, B.; Lefeber, D. Scaling laws of compliant elements for high storage capacity in robotics. *Mech. Mach. Theory* **2019**, *139*, 482–505. [CrossRef]

11. Rezazadeh, S.; Hurst, J.W. On the optimal selection of motors and transmissions for electromechanical and robotic systems. In Proceedings of the IEEE/RSJ International Conference on Intelligent Robots and Systems, Chicago, IL, USA, 14–18 September 2014; pp. 4605–4611.
12. Verstraten, T.; Mathijssen, G.; Furnémont, R.; Vanderborght, B.; Lefeber, D. Modeling and design of geared DC motors for energy efficiency: Comparison between theory and experiments. *Mechatronics* **2015**, *30*, 198–213. [CrossRef]
13. Verstraten, T.; Furnémont, R.; Mathijssen, G.; Vanderborght, B.; Lefeber, D. Energy consumption of geared DC motors in dynamic applications: Comparing modelling approaches. *IEEE Robot. Autom. Lett.* **2016**, *1*, 524–530. [CrossRef]
14. Bartlett, H.L.; Lawson, B.E.; Goldfarb, M. Optimal transmission ratio selection for electric motor driven actuators with known output torques and motion trajectories. *J. Dyn. Sys. Control* **2017**, *139*, 101013. [CrossRef]
15. Pasch, K.A.; Seering, W.P. On the drive systems for high performance machines. *J. Mech. Trans. Autom. Des.* **1984**, *106*, 102–108. [CrossRef]
16. Van de Straete, H.J.; De Schutter, J.; Degezelle, P.; Belmans, R. Servo motor selection criterion for mechatronic applications. *IEEE-ASME Trans. Mechatron.* **1998**, *3*, 43–50. [CrossRef]
17. Van de Straete, H.J.; De Schutter, J.; Belmans, R. An efficient procedure for checking performance limits in servo drive selection and optimization. *IEEE-ASME Trans. Mechatron.* **1999**, *4*, 378–386. [CrossRef]
18. Cusimano, G. Optimization of the choice of the system electric drive-transmission for mechatronic applications. *Mech. Mach. Theory* **2007**, *42*, 48–65. [CrossRef]
19. Giberti, H.; Cinquemani, S.; Legnani, G. Effects of transmission mechanical characteristics on the choice of a motor-reducer. *Mechatronics* **2010**, *20*, 604–610. [CrossRef]
20. Giberti, H.; Cinquemani, S.; Legnani, G. A practical approach to the selection of the motor-reducer unit in electric drive systems. *Mech. Based Des. Struct. Mach.* **2011**, *39*, 303–319. [CrossRef]
21. Cusimano, G. Choice of the electrical motor and transmission in mechatronic applications: The torque peak. *Mech. Mach. Theory* **2011**, *46*, 1207–1235. [CrossRef]
22. Cusimano, G. Influence of the reducer efficiencies on the choice of motor and transmission: Torque peak of the motor. *Mech. Mach. Theory* **2013**, *67*, 122–151. [CrossRef]
23. Cusimano, G. Choice of motor and transmission in mechatronic applications: Non-rectangular dynamic range of the drive system. *Mech. Mach. Theory* **2015**, *85*, 35–52. [CrossRef]
24. Cusimano, G. Non-rectangular dynamic range of the drive system: A new approach for the choice of motor and transmission. *Machines* **2019**, *7*, 54. [CrossRef]
25. Cusimano, G.; Casolo, F. An almost comprehensive approach for the choice of motor and transmission in mechatronic applications: Motor thermal problem. *Mechatronics* **2016**, *40*, 96–105. [CrossRef]